JOURNAL OF CATALYSIS 56, 110–118 (1979)

Analysis of Thermal Desorption Curve for Heterogeneous Surfaces

II. Nonlinear Variations of Activation Energy of Desorption

YASUO TOKORO, TOSHIO UCHIJIMA, AND YUKIO YONEDA

Department of Synthetic Chemistry, Faculty of Engineering, The University of Tokyo, Hongo, Bunkyo-ku, Tokyo 113, Japan

Received December 12, 1977; revised July 21, 1978

We reported analyses of the desorption curve for the simple heterogeneous surface. This paper deals with the more general heterogeneous surface with nonlinear variation of energy of desorption as a function of surface coverage. Computer simulation shows that the characteristic changes of the curve shapes are caused by variations of the distribution pattern of the activation energy of desorption. Thus, the determination of the profile of $E_d(\theta)$ is possible by the analysis of the peak shape with a few assumptions; the rate parameters, $E_d(\theta)$ and A, of desorption can be deduced as a function of surface coverage, θ, by solving a number of simultaneous equations

$$E_d(\theta) - RT \ln A = RT \ln (\theta^n/\beta C),$$

where n is the order of desorption, β is the heating rate, C is the normalized concentration, A is the frequency factor, and $E_d(\theta)$ is the activation energy of desorption, assuming the relation

$$E_d(\theta) = \sum_{k=0}^{N} \alpha_k (1 - \theta)^k.$$

The above analysis was verified by its application to the various simulated desorption curves. The thermal desorption curves of oxygen on ZnO and silver catalyst were analyzed by this method and found to give the reliable values of rate parameters of desorption as a function of the surface coverage; $E_d(\theta)$ varying from 21.5 ± 1.5 kcal/mol at the initial stage of desorption to 32.0 ± 3.0 kcal/mol at the end for ZnO and from 28.5 ± 0.5 to 35.0 ± 0.5 kcal/mol for silver catalyst. The result was much more improved by the simultaneous analysis of the plural desorption curves obtained at different heating rates.

INTRODUCTION

The thermal desorption technique has been commonly used for studies of chemisorbed states on metal surfaces (*1*). In some cases of single-crystal planes of metals, thermal desorption curves can be assumed to be those obtained from a homogeneous surface and analyzed easily to give the rate parameters of desorption, i.e., frequency factor and activation energy, although caution is needed (*2*). Nevertheless, the thermal desorption technique may be useful for characterizing such surfaces in cooperation with other techniques, e.g., LEED, AES, and work function measurements (*3–5*). Thermal desorption of gas from polycrystalline metals, metal oxides, and even single crystals of various metals usually yields a curve with multiple peaks and/or a complicated shape, which is quite different from that obtained from a homogeneous surface. This may be due in part to surface heterogeneity, which has often been claimed

0021-9517/79/010110-09$02.00/0

on the basis of studies of the isothermal chemisorption or the work function (*6*, *7*). Therefore, it is really important to develop a quantitative analysis of heterogeneous surfaces, since surface heterogeneity has been reported to play an important role in several kinds of catalyses (*8*, *9*).

Several authors (*2*, *10*, *11*) have reported analyses of the thermal desorption curve from the simple heterogeneous surface in which the activation energy of desoprtion changes linearly with surface coverage. We also developed independently the analyses for the same kind of surface. The empirical equations for estimation and the curve-fitting method were applied to the simulated curves and to the thermal desorption curve of CO_2 on TiO_2. They are found to be useful and reliable (*12*).

Since many catalysts are supposed to have more complex energy distribution of surface sites, which cannot be approximated by a simple heterogeneity, these analyses (*12*) should be extended to those applicable to a more general heterogeneous surface with nonlinear variation of the activation energy of desorption. The present paper will consider such analyses. Computer simulation shows that the characteristic changes of curve shapes are caused by variations of the distribution pattern of the activation energy of desorption. Within a stated uncertainty, the rate parameters of desorption can be deduced as a function of the surface coverage by obtaining numerical solutions from experimental shapes using the least-squares method.

This type of analysis is applied to the thermal desorption curves of oxygen on zinc oxide and silver catalysts and is verified as useful and reliable. Another method proposed by King (*13*) is compared with this analysis from the viewpoint of practical use.

THEORY AND CALCULATIONS

Simulations

In the case where only a single adsorbed state exists and no readsorption occurs, the desorption rate is expressed by

$$-d\theta/dT = (A(\theta)/\beta)\cdot\theta^n \cdot\exp(-E_d(\theta)/RT), \quad (1)$$

where β is the heating rate from $T = T_0 + \beta t$, θ is the surface coverage, and n is the order of desorption. In the case of heterogeneous surfaces, the frequency factor, $A(\theta)$, and the activation energy of desorption, $E_d(\theta)$, depend on θ. The desorption rate, $-d\theta/dt$, is equivalent to the partial pressure or the concentration, C, of desorbed molecules normalized by the experimental constants such as a saturated amount of adsorption, a pumping speed, or a carrier gas flow rate, and so on (*14*). Equation (1) is an ordinary differential equation which can be solved numerically for different sets of values of the rate parameters and the heating rate to give the simulated thermal desorption curves (*15*).

In our previous studies (*12*), the simulation curves have been obtained in the case where A is independent of θ and $E_d(\theta)$ changes linearly with θ. It was shown that the maximum rate of desorption shifts to higher temperatures with a decrease in the value of A or an increase in the value of E_d, the peak width becomes broader with a decrease in the value of A, and the peak shape becomes broad and flat with an increase in α with the relation as $E_d(\theta) = E_d^0 + \alpha(1 - \theta)$. These results are qualitatively similar to those reported in Ref. (*2*) for a single adsorbed state.

We are going to deal with the more general heterogeneous surface with nonlinear variation of $E_d(\theta)$ as a function of θ. Thus, the desorption curves were simulated with the constant value of A, 10^{13} s^{-1} and with $E_d(\theta)$ given as various functions of θ, ranging from 30 to 40 kcal mol^{-1} (30 kcal $mol^{-1} \approx 126$ kJ mol^{-1}, 40 kcal $mol^{-1} \approx 167$ kJ mol^{-1}), using the same procedure as reported before (*12*). The values of 10 and 20 K/s were used for β for the cases where $n = 1$ and $n = 2$, respectively.

Determination of the Rate Parameters

The following procedures were used to analyze the desorption curve to obtain the rate parameters as a function of θ.

Equation (1) was transformed to

$$E_d(\theta_i) - RT_i \cdot \ln A_i = RT_i \cdot \ln (\theta_i^n/\beta C_i), \quad (2)$$

where every variable with subscript i corresponds to the value at the ith infinitesimal region of coverage θ. To deal numerically with the various patterns of distribution of $E_d(\theta)$, $E_d(\theta_i)$ is given by

$$E_d(\theta_i) = \sum_{k=0}^{N} \alpha_k (1 - \theta_i)^k, \quad (3)$$

where α_k's have the dimension of energy, kilocalories per mole, but no physical meaning, k is an integer, and N is an integer which gives the most proper distribution function for the $E_d(\theta)$ as shown later. A_i in Eq. (2) is assumed to be constant, i.e., $A_i = A$.

The value of C_i is determined by normalizing the real concentration to satisfy the following relation:

$$\sum_{i=1}^{m} C_i = 1 \quad \text{or} \quad \int_0^{\infty} C dT = 1. \quad (4)$$

The value of θ_i is obtained from

$$\theta_i = 1 - \sum_{i=1}^{i} C_i \quad \text{or} \quad \theta_i = 1 - \int_0^{T_i} C dT. \quad (5)$$

If the desorption curve is divided into $m + 1$ sections at small intervals of temperature (usually $m = 600$), m sets of empirical data (T_i, C_i, θ_i) are obtained by Eqs. (4) and (5). Since these sets of data satisfy Eq. (2), we get m simultaneous linear equations which have the form of Eq. (2). The unknown parameters are the coefficients of Eq. (3), α_0 to α_N, and the frequency factor A. The number of unknown parameter is $N + 2$. If $N + 2$ is less than m, the simultaneous equations can be solved numerically using the least-squares method. Then, the distribution of $E_d(\theta)$ as a function of θ can be determined by Eq. (3) using the values of α_0 to α_N obtained.

Although the analysis can be completed in principle as above, a certain precaution is necessary in practice. A large N in Eq. (3) is desirable, generally, to express the various distribution functions of $E_d(\theta)$. However, if N is too large, it could cause the simultaneous linear equations to give a singular and meaningless solution even if $N + 2$ is less than m.

Thus, the above procedures are repeated in each case from $N = 2$ to $N = 13$, and the desorption curve is simulated using the obtained values of $E_d(\theta)$ and A. The summation of squares of the differences of the observed desorption concentrations, $C_{\text{obs},i}$, and those calculated, $C_{\text{calc}(N),i}$, among the cases from $N = 2$ to $N = 13$ are compared using

$$S_N = \sum_{i=1}^{m} (C_{\text{obs},i} - C_{\text{calc}(N),i})^2. \quad (6)$$

The N value which gives the smallest value of S_N in Eq. (6) is accepted as the most suitable case and is used to calculate the values of $E_d(\theta)$ and A as the final solution. This analysis can be applied to the observed desorption curve by assuming the order of desorption, e.g., 1 or 2.

EXPERIMENTAL

The samples used were zinc oxide (Kadox-15, 10 m^2/g) and silver supported on α-Al_2O_3 (8 wt% Ag) which was prepared by reducing $AgNO_3$ solution with H_2O_2 in NaOH solution, mixing the suspension with α-Al_2O_3 powder, and then drying at 383 K.

The thermal desorption from zinc oxide was carried out in a static system; the catalyst tube was connected to a vacuum system and also to a quadrupole mass spectrometer (Nichiden Varian, NAG-531)

through a variable leak valve. The zinc oxide catalyst (0.1 g) in the tube was treated in oxygen of 21 kPa for 1 h at 723 K and then in vacuum (10^{-4} Pa) for 3 h at the same temperature. The preadsorption was carried out by exposing zinc oxide to oxygen of 21 kPa for 1 h at room temperature. During thermal desorption, the desorbed oxygen from zinc oxide was introduced into the mass spectrometer by pumping it through a variable leak valve. A small time constant (1.5 s) for pumping of this system assures that the observed oxygen pressure is proportional to the desorption rate.

The flow system was used for all procedures on the silver catalyst. The silver catalysts were treated in an oxygen flow for 1 h at 773 K and then in a hydrogen flow for 1 h at the same temperature. Oxygen was adsorbed on the silver catalyst by allowing oxygen to flow through the sample for 1 h at 373 K. Thermal desorption was measured in a He flow using a thermal conductivity cell as a detector. The desorption rate is again proportional to the pressure of the desorbed oxygen.

Thermal desorption curves were obtained using a linear heating schedule at the rate of 4 or 10 K/min (0.067 or 0.167 K/s) from room temperature to 673 K.

RESULTS

Simulations

The distribution profiles of $E_d(\theta)$ used for simulation are shown in curves 1 to 8 in Fig. 1. The thermal desorption curves simulated according to first-order kinetics of desorption are shown in Figs. 2a and b. The curve numbers correspond to those in Fig. 1. The homogeneous surface and the simple heterogeneous surface give the simulated curves 1 and 2, respectively, in Fig. 2a, which are the same ones reported previously, but are shown here again for comparison. In fact, any desorption curve shape can be explained satisfactorily by some combination of curves 1 and 2 in Fig. 2a.

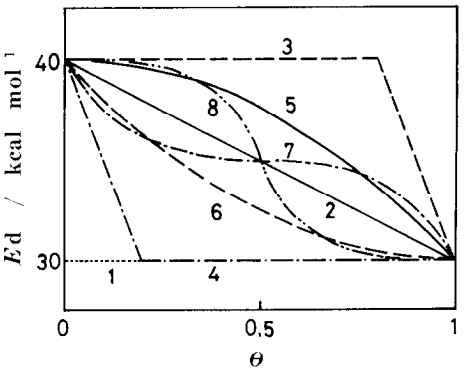

FIG. 1. Distribution profiles of $E_d(\theta)$.

In profiles 3 and 4 in Fig. 1, the surface has the heterogeneous part with steep linear change in $E_d(\theta)$ either at the initial stage of desorption ($\theta > 0.8$) or at the final stage of desorption ($\theta < 0.2$) with the remainder, constant E_d. As shown in the simulated curves 3 and 4 in Fig. 2a, the thermal desorption occurs as a broad and flat peak in accord with the steep change in $E_d(\theta)$ and as a sharp peak corresponding to the part of constant E_d.

In profiles 5 and 6 in Fig. 1, $E_d(\theta)$ changes gradually with θ, but their trends are rather similar to those of profiles 3 and 4. Thus, desorption curves 5 and 6 in Fig. 2b have shapes similar to those of curves 3 and 4 in Fig. 2a, respectively. The difference in shape between the first and the second peak becomes less pronounced in curves 5 and 6 because the simulated adsorption is more heterogeneous.

The first half of profile 7 (Fig. 1) is similar to profile 3 and the last half is similar to profile 4. The shape of desorption curve 7 (Fig. 2b) can be explained as a kind of combination of desorption curves 3 and 4. The shape of curve 8 (Fig. 2b) can be also explained in the same way as a combination of profiles 4 and 3 in this sequence.

In the case of second-order kinetics of desorption, the simulated desorption curves

are similar in shape to those of first-order kinetics, except that second-order desorption gives a broader curve than first-order desorption and maximum rate of desorption is shifted to higher temperatures as is shown in Fig. 3 for profile 8 from Fig. 1.

As shown above, characteristic changes in desorption peak shape occur for different distribution profiles of $E_d(\theta)$. Thus, determination of the profile of $E_d(\theta)$ by analysis of the peak shape is possible. We have to assume the order of desorption as 1 or 2 for this analysis, since both the order, n, and the profile of $E_d(\theta)$ have some effects on the peak shape, and it is difficult to determine the order, n, independently by discriminating both effects.

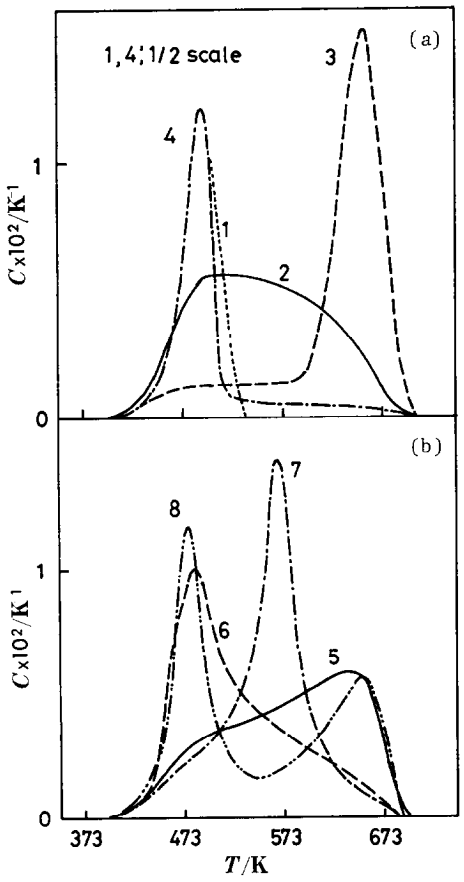

FIG. 2. Thermal desorption curves simulated according to first-order kinetics: $A = 10^{13}$ s^{-1}, $\beta = 10$ K/s.

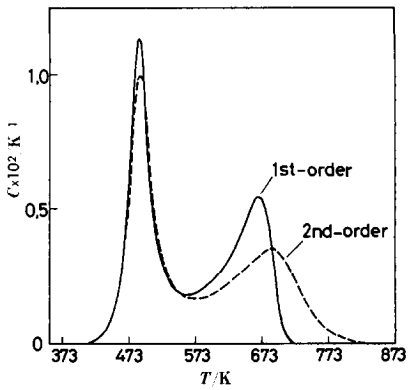

FIG. 3. Comparison between thermal desorption curves simulated according to first- and second-order kinetics: $A = 10^{13}$ s^{-1}, $\beta = 20$ K/s.

Determination of the Rate Parameters

(*i*) *Analysis of the simulated desorption curves.* We applied the analysis explained in the previous section to the simulated desorption curves in Fig. 2. The values of $E_d(\theta)$ and A obtained by the analysis showed good agreement with input values used for simulations in all cases. The maximum deviation was about 5% in the case of first-order desorption over the entire range of θ and through all the heterogeneous profiles. Second-order desorption showed a maximum deviation of about 8%. These deviations are caused mainly by the fact that some distribution profiles of $E_d(\theta)$ are too complex to be expressed as the linear combination of the power terms of $(1 - \theta)$. However, an order of magnitude of 5 or 8% deviation is not so large in this kind of analysis. Thus, this analysis can be applied to the desorption curve obtained with enough experimental caution, based on the assumptions that the frequency factor is independent of surface coverage and the order of desorption is first or second.

(*ii*) *Analysis of the experimental desorption curves.* The thermal desorption curves of oxygen from zinc oxide are shown in Fig. 4. Each curve has a sharp peak with two small shoulders around 373 and 573 K,

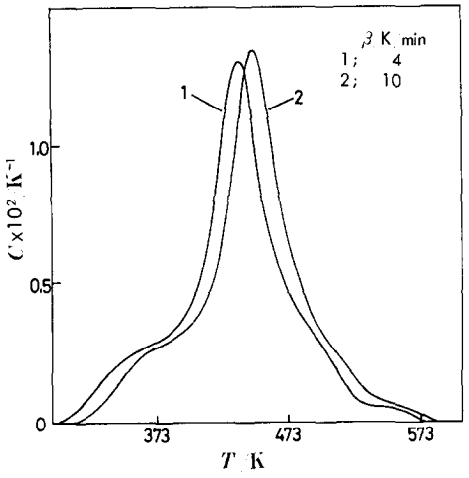

FIG. 4. Thermal desorption curves of oxygen on zinc oxide.

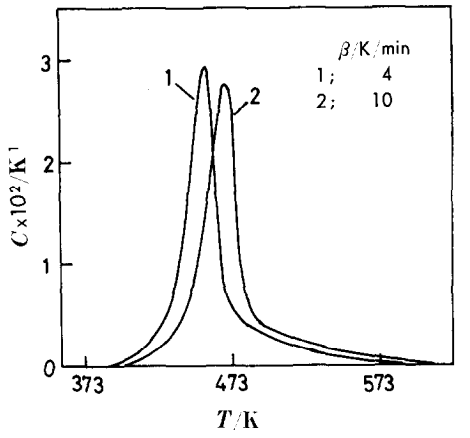

FIG. 6. Thermal desorption curves of oxygen on silver catalysts.

and the shapes are quite similar to that of curve 7 in Fig. 2b. The peak temperatures of these curves agree well with those reported by Tanaka and Blyholder (*16*), who also reported that the adsorbed oxygen species is a superoxide. Hence, it is justified to assume that these peaks correspond to the desorption of the superoxide which should follow first-order kinetics. Figure 5 shows the results obtained by the analyses of these curves using first-order kinetics. The other several independent runs also showed good reproducibility in the values of $E_d(\theta)$ and A. The values of $E_d(\theta)$ vary from 20 to 23 kcal mol^{-1} at the initial stage of desorption to 29 to 35 kcal mol^{-1} at the end, following a shape similar to profile 7 in Fig. 1. The value of A was $10^{9.5-11.1}$ s^{-1}.

The thermal desorption curves of oxygen from the silver catalyst are shown in Fig. 6. Each curve consists of a sharp peak around 450 to 470 K with a small broad tail from 520 to 580 K. Figure 7 shows the results of the analysis assuming

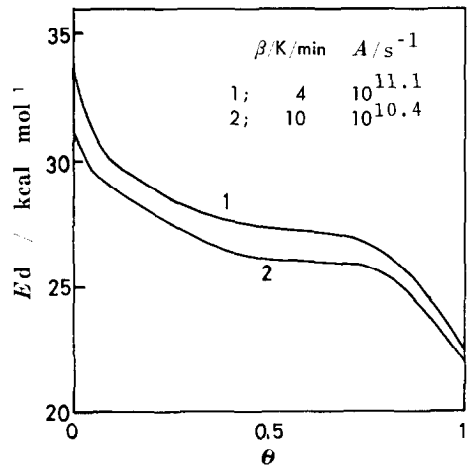

FIG. 5. Results obtained by the analysis of thermal desorption curves of oxygen on zinc oxide.

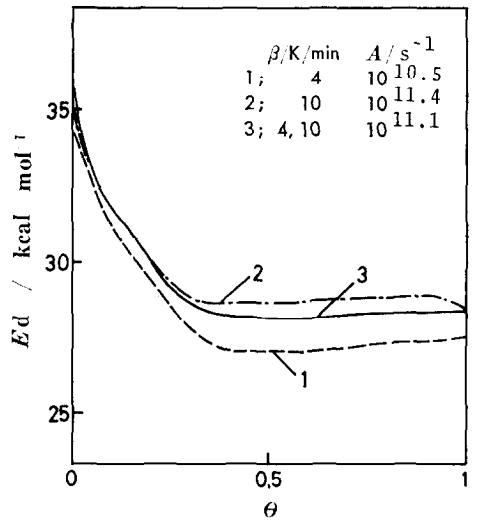

FIG. 7. Results obtained by analysis of thermal desorption curves of oxygen on silver catalysts.

first-order desorption. The value of $E_d(\theta)$ changes from 28–29 to 35 kcal mol^{-1} following a shape similar to profile 4 in Fig. 1, and the value of A is $10^{10.5-11.4}$ s^{-1}. Alternatively, an analysis was also made on the assumption of second-order desorption, but it gave unreasonable results in the sense that the value of $E_d(\theta)$ became considerably smaller as desorption proceeded, and, also, the simulated curve obtained by using these results did not reproduce the observed one well. Hence, at least the main part of the desorption curve should follow first-order kinetics. This result does not agree with that by Kollen and Czanderna (*17*) who showed that desorption was second order on silver powder. This disagreement may stem from the difference in the nature of the preparations.

The main peak of the curve in Fig. 6 has a shape quite close to that from a homogeneous surface. This is in accord with the result that $E_d(\theta)$ has an almost constant value up to $\theta \approx 0.6$. Thus the conventional method (*14*) was also applied to the desorption curves, which are different in the heating rate, assuming a homogeneous surface. The results are 31 kcal mol^{-1} for E_d and $10^{13.3}$ s^{-1} for A, which are rather close to the above results, hereby confirming the reliability of the analysis in this study.

Several authors (*18–21*) have reported E_d values for oxygen desorption on silver as determined by isothermal and nonisothermal techniques. These are summarized in Table 1, together with the present result, and show relatively good agreement with each other. The discrepancy may be due to the difference in the nature of the preparations, the pretreatments, and the adsorption temperatures. It is important to determine which adsorbed species of oxygen, molecular or atomic oxygen, is effective in the formation of ethylene oxide in the oxidation of ethylene on silver catalysts. It should be of much interest to examine the reactivity and selectivity of these surface oxygen species to ethylene. The present authors are currently working on this subject.

TABLE 1

Reported Values for E_d of Oxygen Desorption on Silver

Authors	E_d (kcal mol^{-1})
Benton and Drake (*18*)	28.4
Sandler and Durigon (*19*)	32.5
Kilty and Sachtler (*20*)	34
Kollen and Czanderna (*17*)	35
Rovida *et al.* (*21*)	35–40
Present paper	28.6–35.8

DISCUSSION

A few authors have reported the analysis of thermal desorption curves for heterogeneous surfaces. Petermann (*1*) and Winterbottom (*22*) discussed the analysis for patches of several different adsorbed states. King (*13*) reported the analysis for a heterogeneous surface where virtually a continuous distribution of adsorbed states exists and named it "the complete analysis."

From a set of desorption curves obtained on the surfaces of different initial coverages, an Arrhenius plot of ln (desorption rate) versus $1/T$ can be obtained at any constant coverage θ_k. Thus, the slope gives the value of $E_d(\theta)$ at θ_k. Repeating this procedure at many different values of θ_k, $E_d(\theta)$ can be obtained as a function of θ. The intercept of the Arrhenius plot gives $\ln A(\theta) + n \cdot \ln \theta$. If the plot of this term versus $\ln \theta$ gives a straight line, the order of desorption is obtained by the slope, and the value of A is obtained by the intercept as a constant value independent of θ. If $\ln A(\theta) + n \cdot \ln \theta$ has a nonlinear relation with $\ln \theta$, the value of n should be obtained by another method to determine $A(\theta)$ as a function of θ.

King has never reported the practical

application. Falconer and Madix (*23*) applied King's method to the simulated curves where $E_d(\theta)$ changes linearly from 30 to 32 kcal mol^{-1} and obtained the satisfactory result within the coverage of 0.04 to 0.3. We also tried to apply his method to the simulated curves from the simple heterogeneous surface of $E_d(\theta)$ from 30 to 40 kcal mol^{-1}. The values of $1/T$ at constant coverages θ_k's were found to be very close to each other. A large error is involved in the Arrhenius plot, especially at higher coverage. At higher coverage, it is necessary to measure the temperature with accuracy within 0.1°C in order to make a reliable analysis, but it is difficult to realize this condition.

Next, we developed a new modified method, which uses many desorption curves obtained at different heating rates instead of different initial coverages. If the order of desorption could be determined by other methods, the values of ln $(C_k \cdot \beta/\theta_k{}^n)$ obtained from the curves of different heating rates can be plotted against $1/T$ at any constant coverage θ_k. $E_d(\theta)$ and $A(\theta)$ at θ_k can be obtained from the slope and the intercept of this plot. Repeating this procedure at many different coverages θ_k's, $E_d(\theta)$ and $A(\theta)$ are obtained as functions of θ. As a result of the application of this method to the simulated curves, accurate results were obtained when the heating rate was changed by the order of magnitude of 10^2. This method is excellent in the sense that one is not required to assumed that $A(\theta)$ is independent of θ, although it is difficult to realize such a large change in β without involving much difference in temperature distribution in the catalyst bed.

In contrast with the above two methods which require many runs, the analysis in this study requires only one desorption run in principle. This can be called the single curve analysis. The single curve analysis may be accompanied by some problems because not only are experimental errors unavoidable in any single run but also the different sets of values of $E_d(\theta)$ and A could sometimes reproduce well the same desorption curve. In fact, the values of $E_d(\theta)$ and A shown for cases 1 and 2 in Fig. 7 can reproduce the respective desorption curves obtained at $\beta = 4$ and 10 K/min, but differ from each other by about 10%. One set of the values of the rate parameters cannot reproduce well the observed desorption curve obtained at different β values, and vice versa. We applied the analysis in this study to the two observed curves in Fig. 6 simultaneously, and the values obtained for $E_d(\theta)$ and A are plotted as case 3 in Fig. 7. These values can reproduce both observed curves very well. Hence, the analysis in this study becomes much more improved when applied simultaneously to the plural desorption curves obtained at different heating rates than to the single curve.

The present study provides a practical and reliable method for obtaining the distribution of the activation energy of desorption by analysis of the shape of the thermal desorption curve on the basis of a few assumptions.

ACKNOWLEDGMENT

Financial support in part by the Kawakami Foundation is gratefully acknowledged.

REFERENCES

1. Petermann, L. A., "Progress in Surface Science," Vol. 3, p. 1. Pergamon Press, London/New York, 1972.
2. Czanderna, A. W., Biegen, J. R., and Kollen, W., *J. Colloid Interface Sci.* **34**, 406 (1970).
3. May, J. W., "Advances in Catalysis," Vol. 21, p. 151. Academic Press, New York, 1970.
4. Ehrlich, G., "Advances in Catalysis," Vol. 14, p. 255. Academic Press, New York, 1963.
5. Pentenero, A., *Catal. Rev.* **5**, 199 (1972).
6. Boreskov, G. K., Popovskii, V. V., and Sazonov, V. A., *Proc. Int. Congr. Catal., 4th, Moscow*, 33 (1968).
7. Barford, B. D., and Rye, R. R., *J. Chem. Phys.* **60**, 1036 (1974).

8. Uchijima, T., and Yoneda, Y., *Bull. Chem. Soc. Japan* **47**, 2181 (1974).
9. Sachtler, W. M. H., Dorgelo, G. J. H., Fahrenfort, J., and Voorhoeve, R. J. H., *Proc. Int. Congr. Catal. 4th, Moscow*, 34 (1968).
10. Carter, G., *Vacuum* **12**, 245 (1962).
11. Dawson, D. T., and Peng, Y. K., *Surface Sci.* **33**, 565 (1972).
12. Tokoro, Y., Misono, M., Uchijima, T., and Yoneda, Y., *Bull. Chem. Soc. Japan* **51**, 85 (1978).
13. King, D. A., *Surface Sci.* **47**, 384 (1975).
14. Cvetanović, R. J., and Amenomiya, Y., "Advances in Catalysis," Vol. 17, p. 103. Academic Press, New York, 1967.
15. Redhead, P. A., *Vacuum* **12**, 203 (1962).
16. Tanaka, K., and Blyholder, G., *J. Phys. Chem.* **76**, 3184 (1972).
17. Kollen, W., and Czanderna, A. W., *J. Colloid Interface Sci.* **38**, 152 (1972).
18. Benton, A. F., and Drake, L. C., *J. Amer. Chem. Soc.* **56**, 255 (1934).
19. Sandler, Y. L., and Durigon, D. D., *J. Phys. Chem.* **69**, 4201 (1965).
20. Kilty, P. A., and Sachtler, W. M. H., *Catal. Rev.* **8**, 1 (1974).
21. Rovida, G., Pratesi, E., Maglietta, M., and Ferroni, E., *Surface Sci.* **43**, 230 (1974).
22. Winterbottom, W. L., *J. Vac. Sci. Technol.* **9**, 936 (1972).
23. Falconer, J. L., and Madix, R. J., *J. Catal.* **48**, 262 (1977).